J Biomol NMR (2009) 43:1–10
DOI 10.1007/s10858-008-9284-9

ARTICLE

An improved ultrafast 2D NMR experiment: Towards atom-resolved real-time studies of protein kinetics at multi-Hz rates

Maayan Gal · Thomas Kern · Paul Schanda · Lucio Frydman · Bernhard Brutscher

Received: 4 September 2008 / Accepted: 6 October 2008 / Published online: 4 November 2008

Abstract Multidimensional NMR spectroscopy is a well-established technique for the characterization of structure and fast-time-scale dynamics of highly populated ground states of biological macromolecules. The investigation of short-lived excited states that are important for molecular folding, misfolding and function, however, remains a challenge for modern biomolecular NMR techniques. Off-equilibrium real-time kinetic NMR methods allow direct observation of conformational or chemical changes by following peak positions and intensities in a series of spectra recorded during a kinetic event. Because standard multidimensional NMR methods required to yield sufficient atom-resolution are intrinsically time-consuming, many interesting phenomena are excluded from real-time NMR analysis. Recently, spatially encoded ultrafast 2D NMR techniques have been proposed that allow one to acquire a 2D NMR experiment within a single transient. In addition, when combined with the SOFAST technique, such ultrafast experiments can be repeated at high rates. One of the problems detected for such ultrafast protein NMR experiments is related to the heteronuclear decoupling during detection with interferences between the pulses and the oscillatory magnetic field gradients arising in this scheme. Here we present a method for improved ultrafast data acquisition yielding higher signal to noise and sharper lines in single-scan 2D NMR spectra. In combination with a fast-mixing device, the recording of ^{1}H–^{15}N correlation spectra with repetition rates of up to a few Hertz becomes feasible, enabling real-time studies of protein kinetics occurring on time scales down to a few seconds.

Keywords Spatially encoded NMR · Ultrafast acquisition · Multidimensional NMR · Real-time NMR · Hydrogen exchange · Single-transition spin state

M. Gal · L. Frydman (✉)
Department of Chemical Physics, Weizmann Institute of Science, Rehovot 76100, Israel
e-mail: lucio.frydman@weizmann.ac.il

T. Kern · B. Brutscher (✉)
Institut de Biologie Structurale, Jean-Pierre Ebel C.N.R.S.-C.E.A.-UJF 41, rue Jules Horowitz, Grenoble Cedex 38027, France
e-mail: bernhard.brutscher@ibs.fr

P. Schanda
Laboratorium fuer Physikalische Chemie ETH Hoenggerberg, Zurich, CH 8093, Switzerland

Introduction

Multidimensional nuclear magnetic resonance (NMR) spectroscopy is a widely used tool for high-resolution studies of biomolecular structure and dynamics in solution. While fast time-scale dynamics (ps to ms) are accessible via the measurement of spin relaxation rates (Jarymowycz and Stone 2006; Mittermaier and Kay 2006) or residual dipolar coupling constants (Blackledge 2005), kinetic molecular processes taking place on longer time scales can be followed by monitoring NMR spectral changes in real time during a molecular reaction such as protein (un)folding (Zeeb and Balbach 2004; Van Nuland et al. 1998). In the past, atom-resolved real-time NMR studies of kinetic processes in proteins on the seconds, and sub-seconds timescales, have been almost impossible because of the time requirements associated with the recording of multidimensional correlation spectra on macromolecules. In standard 2D NMR only the so-called t_2 time axis is acquired directly, like in 1D NMR, while the additional time axis is

monitored as a discrete incrementation of a time variable (t_1) throughout a series of repetitions (scans) of the basic experiment. Hence, a major disadvantage of 2D NMR is the long acquisition time that, regardless of sensitivity considerations, may be needed for obtaining these spectra.

Over the last years, several conceptually different approaches have been proposed for acquiring 2D NMR spectra in a significantly reduced amount of time (Freeman and Kupce 2003; Malmodin and Billeter 2005; Schanda and Brutscher 2005). The most dramatic time reduction is achieved by the so-called "ultrafast" NMR technique that allows the acquisition of 2D (and higher dimensional) NMR spectra within a single scan (Frydman et al. 2002; Shrot and Frydman 2003). In ultrafast NMR the time incrementation of t_1 is replaced by a spatial encoding step, where nuclear spins in the sample are progressively excited according to their position along a spatial coordinate by the use of a magnetic field gradient acting in combination with a frequency swept radiofrequency (rf) pulse. The result of this manipulation is a spatial winding of the spin magnetizations with a position-dependent phase $C\,\Omega_1 z$, where Ω_1 is the resonance frequency of the nuclear spin, C is a spatio-temporal constant depending on the sample length and some user-defined acquisition parameters relating the Ω_1 evolution in a linear way to the spatial coordinate z. This phase modulation, similar to the $\Omega_1 t_1$ phase behavior in a standard experiment, is conserved during any coherent mixing sequence required for correlating different nuclear spins in a 2D experiment. A spatial decoding or unwinding of the resulting helix is achieved during data acquisition by the use of a second magnetic field gradient. This acquisition gradient G_a results in a constructive interference of the spins along the spatial axis of the sample, a spin echo whose position in time along the $k = \gamma \int G_a(t)\mathrm{d}t$ axis depends on the resonance frequency Ω_1 as well as on the strength of G_a. This reading process can be repeated numerous times by oscillating the sign of the readout gradients, thus allowing to monitor a set of indirect time-domain spectra as a function of the t_2 time evolution. Fourier transformation along the t_2 dimension then results in the desired 2D NMR spectrum.

The time resolution of real-time 2D NMR methods, however, not only depends on the acquisition time of a single 2D data set, but also on the rate at which these experiments can be repeated during the kinetic process under investigation. A recycle delay between successive scans is required to allow the nuclear spins to relax towards thermal equilibrium and, in protein NMR spectroscopy, recycle delays of the order of seconds are generally chosen to yield sufficient ^{1}H polarization to be used for the next scan. Recently, experiments have been optimized for fast repetition rates without a loss in experimental sensitivity (signal to noise ratio per unit experimental time) by accelerating the recovery of proton polarization between subsequent scans. An example of this is the SOFAST-HMQC NMR experiment (Schanda and Brutscher 2005; Schanda et al. 2005) that allows the recording of standard time-encoded 2D ^{1}H–^{15}N protein correlation spectra in a few seconds by reducing the recycle delay to a few milliseconds. In SOFAST-HMQC NMR, longitudinal ^{1}H spin relaxation is enhanced (Pervushin et al. 2002) by the use of a small number of band-selective ^{1}H pulses, and ^{1}H steady-state magnetization is further enhanced by Ernst angle excitation (Ernst et al. 1987).

These two complementary ideas, recording a 2D data set in a single scan by spatial frequency encoding, and reducing the repetition rate without compromising sensitivity have been recently combined in the ultraSOFAST-HMQC experiment shown in Fig. 1a (Gal et al. 2007). Although this experiment allowed us to demonstrate the feasibility of acquiring a series of protein ^{1}H–^{15}N spectra at Hz rates, an excess of signal loss related to different aspects of the experiment discussed below was observed, that limits its applicability in the context of real-time studies of molecular kinetics. Moreover, for the short repetition times used for this experiment, the rf load and the pulsed field gradients required for spatial encoding and decoding could easily exceed the duty cycle recommended for an optimum performance of the probe, particularly in the case of cryogenically cooled probes. Challenged by these features, we introduce here, single-transition-state (STS)-ultraSOFAST-HMQC, an experiment that has the same characteristics in terms of minimal experimental times and repetition rates as ultraSOFAST-HMQC, but that overcomes some of the major limitations of the latter. STS-ultraSOFAST-HMQC yields increased sensitivity under fast-pulsing conditions when compared to ultraSOFAST-HMQC. This is demonstrated by the measurement of fast D/H exchange kinetics from a real-time series of ^{1}H–^{15}N spectra recorded at a rate of $\sim$3 Hz.

Ultrafast 2D NMR—without heteronuclear decoupling

Spatially encoded ultrafast NMR experiments generally result in decreased sensitivity when compared to their standard time-evolution based counterparts. Neglecting sensitivity drops arising from non-ideal radiofrequency and gradient pulses, most of these losses can be rationalized by the following: NMR data acquisition in the presence of a magnetic field gradient requires opening of the filter bandwidth to account for the gradient-induced spread in resonance frequencies from spins over the whole sample volume. Given that the noise detected by the receiver increases with the receiver's bandwidth, the overall sensitivity of the experiment strongly depends on the strength of

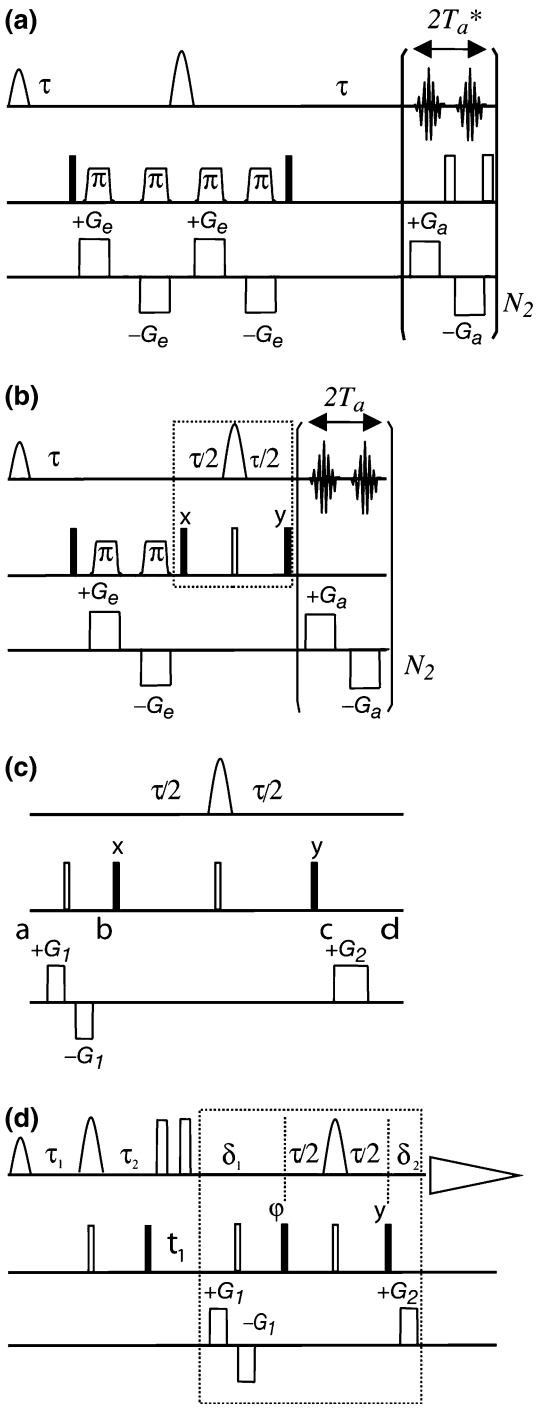

◀ **Fig. 1** NMR pulse sequences used in this study for performing fast 2D ^{1}H–^{15}N correlation experiments of proteins: (**a**) UltraSOFAST-HMQC, (**b**) STS-ultraSOFAST-HMQC, (**c**) the STS pulse sequence element, and (**d**) STS-SOFAST-HMQC. Filled and open pulse symbols indicate 90° and 180° rf pulses, respectively, except for the first ^{1}H pulse that is applied with variable flip angle adjusted for Ernst-angle excitation (Schanda et al. 2005). Unless indicated, all pulses are applied along the x axis. The frequency-chirped pulses used for spatial encoding in the ultrafast sequences (**a**) and (**b**) are achieved by WURST-like amplitude modulation (Kupce and Freeman 1996) suitable for executing 180° nutations (Pelupessy 2003). All selective ^{1}H pulses are typically centered at 8.2 ppm, covering a bandwidth of 4.0 ppm, with the following shapes: PC9 (Kupce and Freeman 1994) for excitation, and REBURP (Geen and Freeman 1991) for refocusing purposes. In all experiments with more than one scan, a simple 2-step phase cycle was applied by inverting the phase of the 90° ^{15}N excitation pulse in concert with the receiver phase. In the STS-ultraSOFAST-HMQC sequence of figure (**b**), ^{1}H chemical shift evolution is not refocused as ultrafast spectra are generally not phased and plotted in absolute-value mode. In sequence (**d**) a pair of ^{1}H 180° broadband inversion pulses (Smith et al. 2001) is applied during the t_1 evolution period. These pulses refocus ^{1}H chemical shift evolution during t_1 without significantly perturbing the polarization of non-amide ^{1}H. The transfer delays τ_1 and τ_2 are set to $\tau_1 = \tau/2 + \delta_1 - \delta_2$ and $\tau_2 = \tau/2 - \delta_1 + \delta_2$. In addition, half the PC9 pulse length has to be subtracted from the τ_1 delay to take into account the effective spin evolution during the PC9 pulse. For Ernst angle excitation, a flip angle $\alpha > 90°$ (typically 120–150°) is required for sequences (**a**) and (**b**), whereas $\alpha < 90°$ (typically 40–60°) is chosen for sequence (**d**)

the acquisition gradients—dictated in turn by spectral widths considerations (see Results). As a consequence, while high magnetic fields provide the high spin polarization and frequency resolution required for (ultra)fast protein NMR methods, the intrinsic per-scan sensitivity of an ultrafast experiment is lower then that of its conventional counterpart.

Different approaches have been proposed in the past to increase this sensitivity aspect of ultrafast NMR, including optimized data acquisition and processing (Gal et al. 2006; Mishkovsky and Frydman 2005). Here we focus on a different source of sensitivity losses, arising from problems related to ^{15}N decoupling during the ^{1}H detection period. Due to the large effective spectral spreads brought about by oscillatory magnetic field gradients during acquisition, heteronuclear decoupling in ultrafast NMR experiments is generally not performed using continuous composite decoupling schemes. Rather, it is realized by 180° high-power refocusing pulses applied at rates SW_H or $2SW_H$, with SW_H the spectral width in the ^{1}H dimension. The finite length of these decoupling pulses, as well as a short gradient recovery delay needed prior to each such pulse, have a direct influence on the required acquisition gradient strength as they reduce the time available for applying a gradient pulse. Owing to this reduced duration, the gradient strength has to be increased in order to cover the same effective spectral width along the spatially encoded dimension. The filter bandwidth, in turn, has to be larger, resulting in a further increase in the detected noise and thus a reduction in sensitivity. ^{15}N decoupling during ^{1}H detection is also the main source of rf probe heating leading to partial probe detuning, increased B_0-field inhomogeneity, and the risk of long-term damage of expensive cryogenic probes (Kern et al. 2008). Due to all these reasons combined, the development of alternative techniques that do not require heteronuclear decoupling during acquisition is of particular interest for ultrafast NMR experiments.

An alternative to heteronuclear decoupling involves the use of spin-state-selective NMR techniques, creating a

single-transition spin state that evolves during the final detection. This results in a single resonance line shifted either upfield or downfield by $\Delta\nu = J_{NH}/2$ with respect to the standard ^{15}N-decoupled spectrum without the need for implementing an active ^{15}N decoupling. Examples of spin-state selection techniques include the S^{3}E (Meissner et al. 1997), double-S^{3}CT (Meissner et al. 1998; Pervushin et al. 1997), and IPAP-type (Ottiger et al. 1998; Andersson et al. 1998) filters. The S^{3}E and double-S^{3}CT sequences require additional 90° rf pulses on the ^{1}H channel, and they are thus incompatible with the SOFAST-HMQC experiment. IPAP is compatible with SOFAST-HMQC but it doubles the minimal experimental time as 2 spectra need to be recorded yielding inphase, and anti-phase doublet lines, respectively. A singlet spectrum is only obtained after appropriate combination of the two data sets as described recently for IPAP versions of SOFAST-HMQC (Schanda et al. 2005; Kern et al. 2008). Here we present a new single-transition-state (STS) filter sequence that yields spin-state selection in the ^{1}H dimension within a single scan. This STS filter element, depicted inside the square line in Fig. 1b, is compatible with both, spatial encoding and SOFAST-HMQC and can therefore be employed without affecting the minimal achievable 2D frame rate.

To better understand the operation of this new approach to coupling-free 2D NMR, we focus first on the STS filter element highlighted in Fig. 1c. Assuming that an initial multiple-quantum spin state $\sigma_a = 2H_yN_x$ has been created at time point a, and neglecting chemical shift evolution, the gradient pulses G_1 induce a winding of the spin polarization along the z-axis yielding a spin state at point b given by:

$$\sigma_b = 2H_yN_x\cos(k_1z) + 2H_yN_y\sin(k_1z) \qquad (1)$$

with the wave number $k_1 = 2\gamma_N\int_0^{\tau_1} G_1(t)\mathrm{d}t$, and τ_1 the gradient length. Between time points b and c, the 2 coherences, $2H_yN_x$ and $2H_yN_y$ then evolve along separate pathways as:

$$(I)\quad 2H_yN_y \xrightarrow{90°N_x} 2H_yN_z \xrightarrow{2\Delta} H_x \xrightarrow{90°N_y} H_x$$

$$(II)\quad 2H_yN_x \xrightarrow{90°N_x} 2H_yN_x \xrightarrow{2\Delta} 2H_yN_x \xrightarrow{90°N_y} 2H_yN_z \qquad (2)$$

After the final gradient pulse G_2 with wave number $k_2 = \gamma_H\int_0^{\tau_2} G_2(t)\mathrm{d}t$, the spin state is given by:

$$\begin{aligned}\sigma_d &= \{H_x\cos(k_1z) + 2H_yN_z\sin(k_1z)\}\exp(ik_2z)\\ &= \{H_x\exp[i(k_1+k_2)z] + H_x\exp[i(-k_1+k_2)z]\}/2 + \{2H_yN_z\exp[i(k_1+k_2)z] - 2H_yN_z[i(-k_1+k_2)z]\}/2i\\ &= (H_x + 2H_xN_z)\exp[i(k_1+k_2)z]/2 + (H_x - 2H_xN_z)\exp[i(-k_1+k_2)z]/2\end{aligned} \qquad (3)$$

The $(H_x + 2H_xN_z)$ and $(H_x - 2H_xN_z)$ operators describe single-transition spin states, corresponding to the upfield and downfield ^{1}H doublet components. Experimentally, one of the doublet components is selected by setting the relative gradient strengths to either $k_2 = -k_1$ or $k_2 = k_1$. The unwanted doublet component stays dephased along the z-axis, and averages to zero when integrating over the whole sample length.

The STS filter element of Fig. 1c can be inserted into the standard SOFAST-HMQC experiment, as well as into the spatially encoded ultraSOFAST-HMQC. In the STS-SOFAST-HMQC experiment of Fig. 1d, the STS block is inserted after the t_1 evolution period. As a consequence, the accumulated phase at time point b is the combination of the ^{15}N chemical shift evolution and the spatial winding, $\Omega_N t_1 + k_1 z$. Assuming $k_2 = -k_1$, the spin state at time point d is then given by:

$$\begin{aligned}\sigma_d^I(t_1) &= (H_x + 2H_xN_z)\exp(i\Omega_N t_1)/2\\ &\quad + (H_x - 2H_xN_z)\exp(-i\Omega_N t_1)\exp(-i2k_1z)/2\end{aligned} \qquad (4)$$

Only the first part of Eq. [4], corresponding to one of the ^{1}H doublet components, yields a detectable signal that is phase modulated as a function of the ^{15}N chemical shift and the incremented t_1 delay. The second part of the density matrix, corresponding to the other ^{1}H doublet component, is dephased along a spatial axis, and does not yield any detectable magnetization. As usual for echo/anti-echo quadrature detection schemes (Palmer et al. 1991), a second experiment is required that yields a negative phase evolution in the t_1 dimension:

$$\begin{aligned}\sigma_d^{II}(t_1) &= (H_x + 2H_xN_z)\exp(-i\Omega_N t_1)/2\\ &\quad + (H_x - 2H_xN_z)\exp(i\Omega_N t_1)\exp(i2k_1z)/2\end{aligned} \qquad (5)$$

This is realized experimentally by inverting the gradient G_2 ($k_2 = k_1$), as well as phase φ of the first 90° ^{15}N pulse in the STS element.

In the STS version of the ultraSOFAST-HMQC experiment (Fig. 1b), the G_1 gradient pulses are replaced by a constant-time spatial-encoding scheme. As a result of the combined action of the pulsed field gradients G_e and the frequency-swept ^{15}N pulses, the wave number of the

effective phase encoding at time point b is given by $k_1 = C\Omega_1$, with $C = t_{1\,\max}/L$, and L the effective sample length. During the acquisition gradient, data points are sampled as a function of a wave number $k(t) = \gamma_H \int_0^t G_a(t')\mathrm{d}t'$ yielding a readout spin state given by:

$$\sigma(k) = (H_x + 2H_xN_z)\exp(i(C\Omega_N - k(t))z)/2 + (H_x - 2H_xN_z)\exp(i(k(t) - C\Omega_N)z)/2 \quad (6)$$

For the standard ultraSOFAST-HMQC experiment (Fig. 1a) the same time dependence is obtained for spin evolution during acquisition but only the first coherence-transfer pathway of Eq. [2], yielding inphase coherence, contributes to the detected signal. Therefore, from a theoretical point of view, and neglecting the consequences of finite ^{15}N pulse lengths, the standard and STS versions of the ultraSOFAST-HMQC experiment are supposed to provide the same signal intensity—yet freeing the experiment from the need of active ^{15}N decoupling.

Results and discussion

STS-ultraSOFAST-HMQC

An experimental comparison between the performance of a standard (Fig. 1a) and STS (Fig. 1b) version of ultraSOFAST-HMQC 2D NMR is shown in Fig. 2. Let us emphasize again that no additional sensitivity loss is expected from the single-transition-state selection in the STS-ultraSOFAST-HMQC experiment. All data sets were recorded on an 800 MHz spectrometer equipped with a cryogenically cooled probe on a 2.3 mM sample of ^{15}N-labeled ubiquitin, using identical acquisition parameters except for the acquisition gradients, and for the ^{15}N decoupling procedures. The spectrum in panel (a) was obtained using the standard ultraSOFAST-HMQC experiment (Fig. 1a), where ^{15}N decoupling was realized by high-power 180° pulses placed within the $\pm G_a$ transitions and a 10 μs delay was inserted between the G_a gradient and the ^{15}N pulses. In the spectrum of panel (b) this delay was increased to 20 μs; no longer recovery delays were tested, as this would have increased the acquisition gradient strength to a level too high for the experimental setup. The spectrum in Fig. 2c recorded using the STS pulse sequence of Fig. 1b does not require any ^{15}N decoupling. For a fair comparison of spectral line shapes and signal intensities, no post processing such as linear prediction or signal apodization was employed.

A significantly improved spectral quality and signal to noise ratio (SNR) are observed when comparing the STS spectrum against the spectra recorded with the standard ultraSOFAST-HMQC version. The spectra in Fig. 2a and b, display a residual coupling of about ~35 and ~20 Hz, respectively, along the ^{1}H dimension. This is most-likely resulting from magnetic field currents that extend into the $+G_a \leftrightarrow -G_a$ switching times, and spoil the efficiency of the decoupling pulses. The use of a longer delay between the PFG and ^{15}N pulses increases the decoupling performance, but further decreases the sensitivity of the experiment (Fig. 1b). This can be explained by the dependence of the SNR on the strength of the acquisition gradient G_a and its dependence on the duration T_a. In the ultraSOFAST-HMQC experiment the effective spectral width in the F_1 (^{15}N) and F_2 (^{1}H) dimensions are given by $SW_N(F_1) = \frac{\gamma_H \cdot G_a \cdot T_a \cdot L}{2 \cdot t_1^{\max}}$ and $SW_H(F_2) = \frac{1}{2T_a^*}$, where $T_a^* = T_a + \delta N + \varepsilon$ is half the period of a full acquisition loop

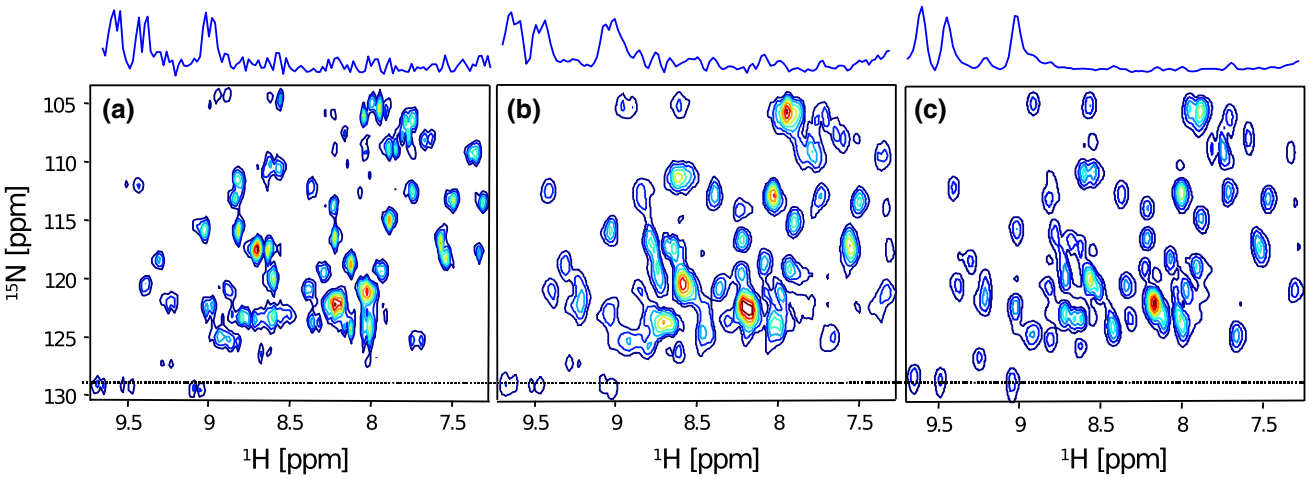

Fig. 2 Sensitivity comparison between standard and STS versions of ultraSOFAST-HMQC. All spectra were acquired on a 800 MHz spectrometer equipped with a cryogenic probe using the following experimental parameter settings: $G_e = 36$ G/cm, $N_2 = 128$, $t_1^{\max} = 12$ ms, $T_a^* = 250$ μs, ^{15}N 180° pulse length = 64 μs, $G_a = 29.3$ G/cm, 33.2 G/cm, and 20.8 G/cm for panels a, b, and c, respectively. The recovery delay between acquisition gradient and ^{15}N 180° pulses was set to (**a**) $\varepsilon = 10$ μs, and (**b**) $\varepsilon = 20$ μs

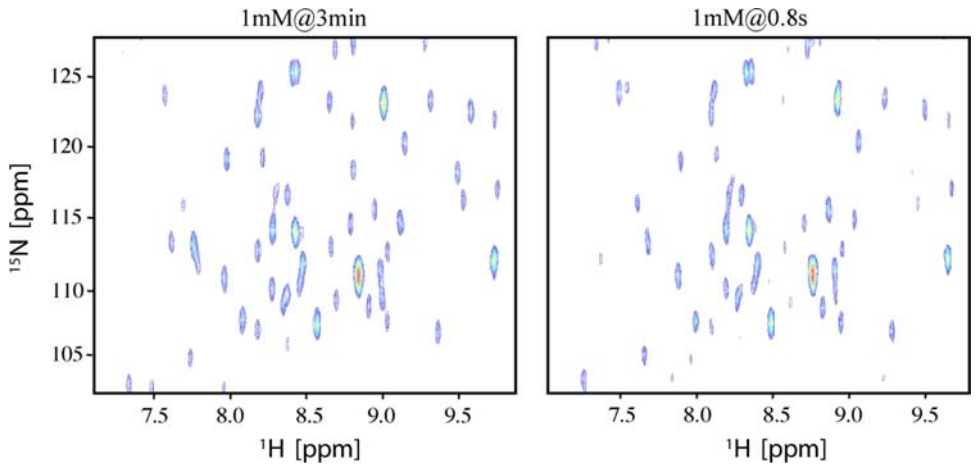

Fig. 3 STS-UltraSOFAST-HMQC spectra acquired on a 800 MHz machine equipped with a cryogenic probe. The spectrum on the right has been recorded in an experimental time of less than 1 s, while a longer acquisition time has been chosen for the left spectrum shown as a reference. Interleaving of 2 acquisitions (scans) with interlaced FT along t_2 was used (Mishkovsky and Frydman 2005). Experimental parameters were: $G_e = 36$ G/cm, $N_2 = 128$, $t_1^{max} = 12$ ms, $T_a{}^* = 250$ µs, ^{15}N 180° pulse = 62 µs, $G_a = 12$ G/cm. The sample concentration and acquisition time are as indicated on top of each panel

including an acquisition gradient, the duration of the ^{15}N π pulse (δN), and the gradient recovery delay (ε). The spectral widths SW_H and SW_N depend on the gyromagnetic ratio of ^{1}H, the sample length L, and the maximum t_1 evolution time t_{1max}. In the absence of ^{15}N decoupling, δN and ε are both equal to 0 and $T_a{}^*$ becomes equal to T_a. If additional ^{15}N decoupling is required, T_a is reduced by an amount $\delta N + \varepsilon$ in order to keep $T_a{}^*$ fixed thus covering the same spectral width $SW_H(F2)$. As a consequence, the strength of the acquisition gradient has to be increased to preserve also the spectral width in F_1. Since the filter bandwidth parameter in ultrafast experiments is directly related to the acquisition gradient strength G_a according to $fb = \gamma_H \cdot G_a \cdot L$, it follows that for increasing G_a the noise level detected by the receiver increases. From these considerations the relative SNR in STS and standard ultraSOFAST-HMQC spectra is expected to follow the relation:

$$\lambda = \frac{SNR\ (\mathrm{STS})}{SNR\ (\mathrm{standard})} = \frac{1}{\sqrt{1 - 2\,(\delta N + \varepsilon)\,SW_H}} \qquad (7)$$

For a typical amide ^{1}H spectral width (SW_H) of 4 ppm, a ^{15}N 180° pulse width of 60 µs, and a recovery delay ε of 40 µs, we calculate expected SNR gains of $\lambda = 1.4$ at 600 MHz, and $\lambda = 1.7$ at 800 MHz. In practice, to reach acceptable acquisition gradient levels, a reduced spectral width and shorter recovery delays need to be chosen. The first results in spectral aliasing in the ^{1}H (F_2) dimension, while the latter yields residual line splitting (see above) due to imperfect decoupling performance. In the spectra of Fig. 2 an average SNR ratio of $\lambda \approx 1.8$ is measured with and without the STS pulse element, in close agreement to the expected gain at 800 MHz. At even higher magnetic field strengths, e.g., 900 MHz the sum of ^{15}N pulse length and recovery delay may exceed the required dwell time in the amide ^{1}H dimension ($T_a = 1/SW_H - 2\,(\delta N + \varepsilon) < 0$). Therefore longer $T_a{}^*$ times would have to be chosen resulting in even more dramatic spectral aliasing. In addition, upon using higher magnetic field strengths stronger ^{15}N decoupling fields are required for the standard version, resulting in partial probe detuning, and consequently in a further decrease of the experimental sensitivity. Therefore STS-ultraSOFAST-HMQC represents a clear improvement in terms of SNR especially for application at high magnetic fields that provide the sensitivity required for ultrafast protein NMR.

As demonstrated in Fig. 3, the increased sensitivity provided by the STS-SOFAST-HMQC experiment allows recording a full ^{1}H–^{15}N correlation spectrum of a moderately concentrated (1 mM) ^{15}N-labeled ubiquitin sample in less than 1 s acquisition time on a 800 MHz NMR spectrometer equipped with a cryogenic probe. The spectra were processed using an interlaced FT along t_2, allowing further reduction of the G_a acquisition gradient strength (Mishkovsky and Frydman 2005). This experiment presents a promising step towards ultrafast real-time 2D NMR measurements of protein samples at millimolar concentration.

STS-SOFAST-HMQC

The STS sequence block of Fig. 1c can also be inserted into a standard SOFAST-HMQC experiment. Although this is not the main focus of the present report, we have set up

an optimized pulse sequence for standard time incremented single-transition-spin-state SOFAST-HMQC shown in Fig. 1d. This experiment is conceptually similar to the recently introduced sensitivity-enhanced (SE) IPAP-SOFAST-HMQC (Kern et al. 2008) where two data sets are recorded and combined to yield a ^{1}H–^{15}N HMQC correlation spectrum without the need of ^{15}N decoupling during detection. Both, the SE-IPAP and STS versions of SOFAST-HMQC benefit from sensitivity enhancement in the sense that both quadrature components present after the t_1 evolution period contribute to the detected NMR signal (see Eqs. [2–5]). The STS-SOFAST-HMQC sequence has the advantage that it does not require combination of 2 different data sets, as a single-transition spin state is created by the action of pulsed field gradients. The drawback of this new experiment is that, because of the gradient-induced phase modulation in t_1, the SNR is reduced by a factor $\sqrt{2}$ with respect to either standard SOFAST-HMQC or sensitivity-enhanced IPAP-SOFAST-HMQC. Still the sensitivity provided by this experiment is sufficient to record 2D correlation spectra of proteins at millimolar concentrations in less than 10 s acquisition time, as demonstrated in Fig. 4 for the 2 globular proteins ubiquitin (8.6 kDa) and the lipoprotein YajG (21 kDa). As can be appreciated from the spectra in Fig. 4, the STS-SOFAST-HMQC experiment yields excellent water suppression in a single scan (per t_1 increment) without any phase cycling. The experiment shows also good performance with respect to the time required to reach steady-state conditions after the creation of fluid turbulences when a fast mixing device is used to initiate a kinetic event inside the NMR magnet. Because the delay between defocusing and refocusing gradient pulses is much shorter in STS-SOFAST-HMQC than in standard SOFAST-HMQC, the performance of STS-SOFAST-HMQC is superior to SOFAST-HMQC and similar to the recently proposed fluid-turbulence-adapted (FTA) SOFAST-HMQC sequence (Schanda et al. 2007).

Fast amide exchange kinetics monitored by ultrafast real-time 2D NMR spectroscopy

To experimentally demonstrate the potential of STS-ultraSOFAST-HMQC for monitoring dynamic events in proteins on a seconds time scale, we have measured fast amide deuterium/hydrogen (D/H) exchange rates in ubiquitin at high pH. After rapidly changing the ^{2}H:^{1}H ratio in the sample's buffer, intensity changes of individual cross peaks were monitored in a series of real time 2D spectra to yield a quantitative measure of D/H exchange rates (Bougault et al. 2004; Schanda et al. 2007). Such amide hydrogen exchange measurements provide atom-resolved information about the (partially) unfolded conformational states of a protein that are present under native conditions, even if they are only populated to minuscule levels. The ability to detect small amounts of unfolded conformations arises from the fact that amide hydrogen atoms are protected from exchange as long as they are hydrogen-bonded or buried within the protein. Therefore, only when the amide hydrogen gets solvent exposed by some local or global unfolding event, it can be replaced by a proton or deuteron from the solvent. One interesting case of amide hydrogen exchange arises when the measured exchange

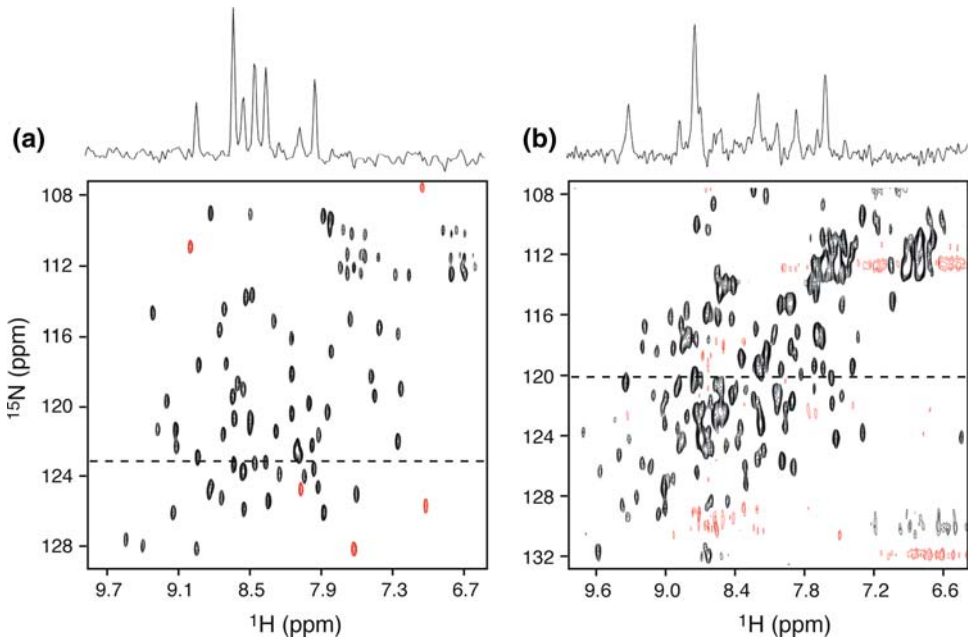

Fig. 4 STS-SOFAST-HMQC spectra recorded on a 800 MHz spectrometer equipped with a cryogenic probe for 0.9 mM samples of (**a**) ubiquitin (8.6 kDa, 25°C), and (**b**) the lipoprotein YajG (20 kDa, 37°C) in experimental times of 4 and 8 s, respectively. Both spectra were recorded with a single scan per t_1 increment, thus without any phase cycling

rates can give direct insight into the kinetics of protein unfolding. This accounts if the intrinsic chemical exchange rate is fast compared to the closing (refolding) rate from an exchange-competent to an exchange-protected conformation. Under these conditions, generally reached at high pH values, exchange is limited by the rate at which an amide site gets exchange-competent, and the NMR-observed exchange rates will thus directly reflect the unfolding rates of the individual residues (Dempsey 2001).

For the D/H exchange experiment shown in Fig. 5, ^{15}N-labeled ubiquitin was dissolved in 90 µl D_2O buffer at pH 12 at a concentration of $\sim$8 mM. The hydrogen exchange reaction was active for a time long enough to ensure complete deuteration of all amide sites in the protein. This solution was then injected into an NMR sample tube containing 350 µl of H_2O buffer that had been placed inside the NMR magnet. The dead time between injection and data acquisition was less than 1 s. After injection the exchange process was followed by recording a series of STS-ultraSOFAST-HMQC spectra with a repetition rate of $\sim 3\ s^{-1}$ (350 ms per 2D spectrum). The peak intensity as a function of exchange time is plotted in Fig. 5a for three distinct amide sites, corresponding to residues T22, I30, and L73. Figure 5b shows the final spectrum after completion of the exchange process (to increase the SNR 128 spectra were added for this spectrum). The peak intensity increases as more and more deuterons get replaced by solvent protons, reaching a

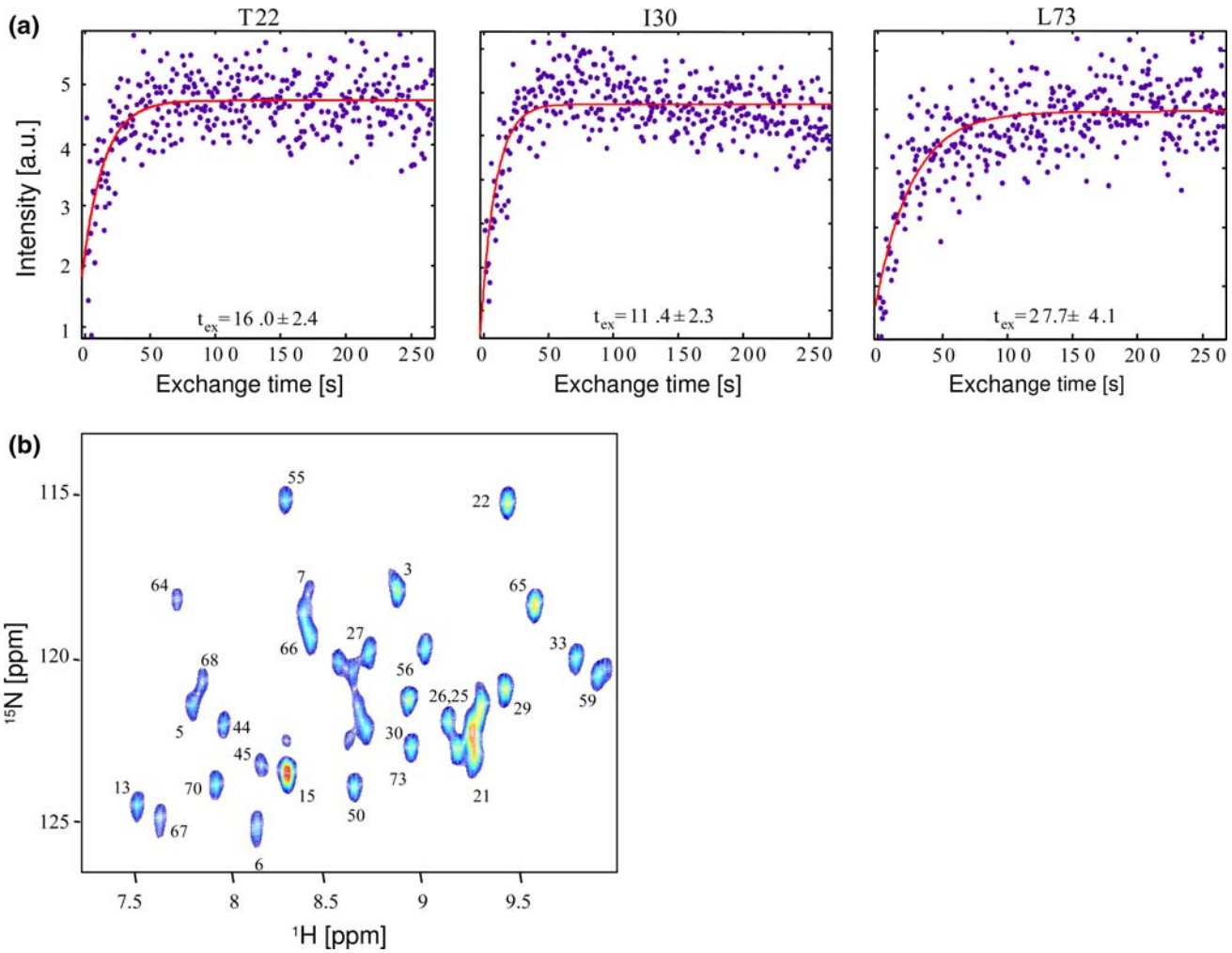

Fig. 5 Amide D/H exchange rates measured on a 600 MHz spectrometer equipped with a cryogenic probe. A series of single-scan STS-ultraSOFAST-HMQC experiments of 350 ms duration per 2D spectrum was recorded to follow the D/H exchange kinetics. Phase cycling was achieved in consecutive 2D acquisitions, as described previously (Schanda et al. 2007), that does not alter the time resolution of the kinetic dimension. Experimental points in (a) reflect peak heights extracted from the STS-ultraSOFAST-HMQC 2D spectra; the t_{ex} exchange lifetimes given in the figure were obtained by fitting of the data points to the equation $I(\tau) = I_0 + I_\infty \cdot \left(1 - \exp\left(-\frac{\tau}{t_{ex}}\right)\right)$. In (b) is shown a reference spectrum acquired as soon as the experiment was finished with the same experimental parameters but with 128 scans

plateau value corresponding to the H_2O/D_2O ratio in solution (in our experiment 3.9:1). This means that although the protein concentration inside the NMR tube was $\sim$1.6 mM, the hydrogenated, and detectable amide sites corresponded to an effective protein concentration of only 1.27 mM.

As the buildup curves in Fig. 5a indicate, the chosen acquisition time of 350 ms per spectrum is a hard test case for the technique in terms of sensitivity and measurement accuracy. Exchange time constants of a second or below can not yet reliably been measured using this technique, although the repetition rate of a few Hz in principle provides access to this time scale. Therefore, the real-time 2D NMR data shown in Fig. 5 should be taken as a proof of principle. It can be foreseen that experimental sensitivity will continue to increase over the next years, and we expect that with this, real-time studies of molecular kinetics at multi-Hz rates will become of practical use. In any case, the STS-ultraSOFAST HMQC experiment presents a step forward towards this aim. Furthermore, and in contrast to previously proposed schemes for fast site-resolved kinetics studies, ultraSOFAST NMR does not require any prior knowledge about peak positions as required for Hadamard spectroscopy (Bougault et al. 2004; Kupce et al. 2003) or extensive spectral aliasing strategies (Lescop et al. 2007).

Conclusions

We have introduced STS-SOFAST-HMQC, a sequence that allows the acquisition of 2D ^{1}H–^{15}N correlation experiments yielding a single cross peak per residue within one scan without heteronuclear decoupling and without the need to record separate in-phase and anti-phase experiments. The full power of this pulse sequence element comes into place when combined with spatial encoding, where the previously applied heteronuclear decoupling using 180° rf pulses leads to significant losses in sensitivity, and decoupling performance is less-than-optimal due to interfering effects from the acquisition gradients. We have shown that well resolved 2D correlation spectra can be obtained at a repetition rate of several Hertz, further extending the time scale accessible to multidimensional real-time kinetic NMR.

Acknowledgments This work was supported by the Commissariat à l'Energie Atomique, the Centre National de la Recherche Scientifique, the University Grenoble1, the French research agency (ANR JCJC05-0077), the European commission (I3, EU-NMR, Contract No. 026145), and the generosity of the Perlman Family foundation. The authors thank Isabel Ayala for help with sample preparation, and Jean-Pierre Simorre for making a sample of the YajG protein available for this study.

References

Andersson P, Weigelt J, Otting G (1998) Spin-state selection filters for the measurement of heteronuclear one-bond coupling constants. J Biomol NMR 12:435–441

Blackledge M (2005) Recent progress in the study of biomolecular structure and dynamics in solution from residual dipolar couplings. Prog Nucl Magn Reson Spectrosc 46:23–61

Bougault C, Feng LM, Glushka J, Kupce E, Prestegard JH (2004) Quantitation of rapid proton–deuteron amide exchange using hadamard spectroscopy. J Biomol NMR 28:385–390

Dempsey CE (2001) Hydrogen exchange in peptides and proteins using NMR-spectroscopy. Prog Nucl Magn Reson Spectrosc 39:135–170

Ernst R, Bodenhausen G, Wokaun G (1987) Principles of nuclear magnetic resonance in one and two dimensions. Oxford University Press, Oxford

Freeman R, Kupce E (2003) New methods for fast multidimensional NMR. J Biomol NMR 27:101–113

Frydman L, Scherf T, Lupulescu A (2002) The acquisition of multidimensional NMR spectra within a single scan. Proc Natl Acad Sci USA 99:15858–15862

Gal M, Mishkovsky M, Frydman L (2006) Real-time monitoring of chemical transformations by ultrafast 2D NMR spectroscopy. J Am Chem Soc 128:951–956

Gal M, Schanda P, Brutscher B, Frydman L (2007) UltraSOFAST HMQC NMR and the repetitive acquisition of 2D protein spectra at Hz rates. J Am Chem Soc 129:1372–1377

Geen H, Freeman R (1991) Band-selective radiofrequency pulses. J Magn Reson 93:93–141

Jarymowycz VA, Stone MJ (2006) Fast time scale dynamics of protein backbones: NMR relaxation methods, applications, and functional consequences. Chem Rev 106:1624–1671

Kern T, Schanda P, Brutscher B (2008) Sensitivity-enhanced IPAP-SOFAST-HMQC for fast-pulsing 2D NMR with reduced radiofrequency load. J Magn Reson 190:333–338

Kupce E, Freeman R (1994) Wide-band excitation with polychromatic pulses. J Magn Reson A 108:268–273

Kupce E, Freeman R (1996) Optimized adiabatic pulses for wideband spin inversion. J Magn Reson A 118:299–303

Kupce E, Nishida T, Freeman R (2003) Hadamard NMR spectroscopy. Prog Nucl Magn Reson Spectrosc 42:95–122

Lescop E, Schanda P, Rasia R, Brutscher B (2007) Automated spectral compression for fast multidimensional NMR and increased time resolution in real-time NMR spectroscopy. J Am Chem Soc 129:2756–2757

Malmodin D, Billeter M (2005) Signal identification in NMR spectra with coupled evolution periods. J Magn Reson 176:47–53

Meissner A, Duus JO, Sorensen OW (1997) Spin-state-selective excitation. Application for E.COSY-type measurement of J(HH) coupling constants. J Magn Reson 128:92–97

Meissner A, Schulte-Herbruggen T, Briand J, Sorensen OW (1998) Double spin-state-selective coherence transfer. Application for two-dimensional selection of multiplet components with long transverse relaxation times. Mol Phys 95:1137–1142

Mishkovsky M, Frydman L (2005) Interlaced Fourier transformation of ultrafast 2D NMR data. J Magn Reson 173:344–350

Mittermaier A, Kay LE (2006) Review—new tools provide new insights in NMR studies of protein dynamics. Science 312:224–228

Ottiger M, Delaglio F, Bax A (1998) Measurement of J and dipolar couplings from simplified two-dimensional NMR spectra. J Magn Reson 131:373–378

Palmer AG, Cavanagh J, Wright PE, Rance M (1991) Sensitivity improvement in proton-detected 2-dimensional heteronuclear correlation NMR-spectroscopy. J Magn Reson 93:151–170

Pelupessy P (2003) Adiabatic single scan two-dimensional NMR spectroscopy. J Am Chem Soc 125:12345–12350

Pervushin K, Riek R, Wider G, Wuthrich K (1997) Attenuated T-2 relaxation by mutual cancellation of dipole–dipole coupling and chemical shift anisotropy indicates an avenue to NMR structures of very large biological macromolecules in solution. Proc Natl Acad Sci USA 94:12366–12371

Pervushin K, Vogeli B, Eletsky A (2002) Longitudinal H-1 relaxation optimization in TROSY NMR spectroscopy. J Am Chem Soc 124:12898–12902

Schanda P, Brutscher B (2005) Very fast two-dimensional NMR spectroscopy for real-time investigation of dynamic events in proteins on the time scale of seconds. J Am Chem Soc 127:8014–8015

Schanda P, Kupce E, Brutscher B (2005) SOFAST-HMQC experiments for recording two-dimensional heteronuclear correlation spectra of proteins within a few seconds. J Biomol NMR 33:199–211

Schanda P, Forge V, Brutscher B (2007) Protein folding and unfolding studied at atomic resolution by fast two-dimensional NMR spectroscopy. Proc Natl Acad Sci USA 104:11257–11262

Shrot Y, Frydman L (2003) Single-scan NMR spectroscopy at arbitrary dimensions. J Am Chem Soc 125:11385–11396

Smith MA, Hu H, Shaka AJ (2001) Improved broadband inversion performance for NMR in liquids. J Magn Reson 151:269–283

Van Nuland NAJ, Forge V, Balbach J, Dobson CM (1998) Real-time NMR studies of protein folding. Acc Chem Res 31:773–780

Zeeb M, Balbach J (2004) Protein folding studied by real-time NMR spectroscopy. Methods 34:65–74